Absolute calibration of Fujifilm BAS-TR image plate response to high energy protons in the range 10-40 MeV

Contact *pmartin21@qub.ac.uk*

P. Martin, H. Ahmed, D. Doria, A. McIlvenny, S. Ferguson, S. Zhai, S. Kar, M. Borghesi

Centre for Plasma Physics, Queen's University Belfast
University Road, Belfast, BT7 1NN

J. Jarrett, P. McKenna

Department of Physics, SUPA, University of Strathclyde
Glasgow, G4 0NG

J. S. Green

Central Laser Facility, Rutherford Appleton Laboratory
Didcot, Oxfordshire, OX11 0QX

Introduction

Imaging Plates (IPs), relying on photo-stimulated luminescence (PSL) are amongst the most popular and reliable detectors for laser driven particle acceleration experiments. IPs are composed of an active layer on top of a magnetic base [1]. The Fujifilm BAS-SR and BAS-MS brands of imaging plate also have a protective layer over the active layer, however the BAS-TR, which this paper will focus on, does not. The active layer is usually composed of europium doped barium fluoride phosphor, $BaFBr_{0.85}I_{0.15}:Eu^{2+}$. When ionizing radiation is incident on the active layer, the above molecule is promoted to an excited, metastable state which can persist for several hours. The state can decay either via spontaneous emission or by stimulated emission when irradiated by light at an appropriate wavelength. Image plate scanners (such as the Fujifilm FLA-5000 used in this experiment) use 633nm laser radiation to stimulate the emission of a 400nm photon, which is then detected and recorded in the scanner as a pixel value, known as a quantum level (QL). A schematic of this process is shown in figure 1 [2].

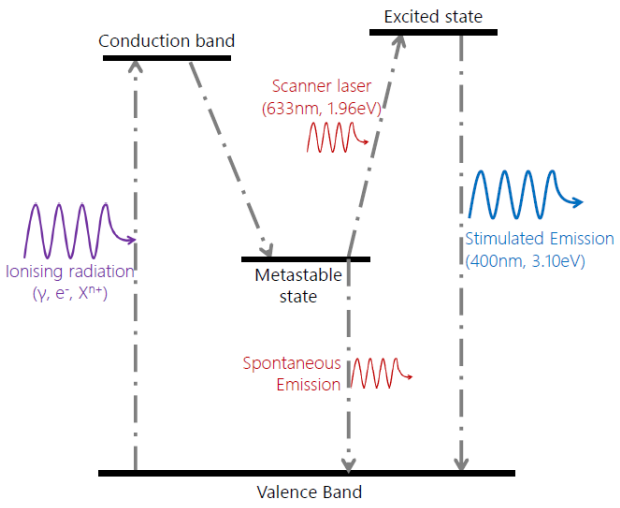

Figure 1: Excitation and Relaxation of metastable state emitting PSL photons

The QL in the scanned image must first be converted to a PSL value before analysis. This is done by using the following formula given by the manufacturer [3],

$$PSL = \left(\frac{R^2}{100}\right) \times \frac{4000}{S} \times 10^{L\times\left(\frac{QL}{2^G-1}-\frac{1}{2}\right)} \quad (1)$$

Where R is the scanning resolution, S is the sensitivity of the scanner, and L is the latitude, and G is the bit depth. In this paper, these values are 25µm, 5000, 5, and 16 bit, respectively.

IPs have several advantages over other detectors, including a high dynamic range, and they can be erased with a bright white light source and reused as long as the active layer remains undamaged. However, one drawback to using image plates is that the signal will fade over time if it is not scanned due to the spontaneous decay of the metastable state. This means the signal must be corrected for the time taken between IP irradiation and scanning. A common practice is to correct the signal to what the PSL value would be at 30 minutes after exposure, given by equation 2 [4],

$$PSL_{30} = \left(\frac{30}{t}\right)^{-0.161} PSL(t) \quad (2)$$

Where t is the time between exposure and scanning in minutes. Due to the wide use of IPs in laser particle acceleration experiments, the need for an absolute calibration of the PSL value to proton number is essential. Thus far, IPs have been calibrated up to 20 MeV in laser acceleration experiments by Mančić *et al* [5] and from 80-200 MeV using a linear accelerator by Rabhi *et al* [6].This paper reports on a calibration effort aiming to fill the above gap in energies.

Another useful method of particle detection is by using Columbia Resin #39, abbreviated to CR-39. This is a solid state nuclear track detector which, when exposed to charged particles and subsequently etched in a 6.5M sodium hydroxide solution at 85°, will reveal the tracks left by each particle in the form of pits on the detector surface [7]. Heavier ions will leave larger pits after etching, enabling the species of ion to be diagnosed by measuring the size of each pit. The key advantage of using this detector is that absolute particle number can be determined by counting each individual pit under a microscope, making it a useful tool for calibration purposes.

Experiment

The calibration was obtained in the course of an experiment performed in Vulcan's Target Area Petawatt (TAP). The primary purpose of the campaign was the investigation of light sail acceleration of ions from ultrathin foils [8]. In calibration shots, after reflection from a plasma mirror, the laser pulse of 1ps duration and 600J energy was focused using an f/3 off-axis parabola, incident normally on a 50nm CH target creating a focal spot of ~5µm FWHM diameter. Taking into account losses in the compressor gratings and plasma mirror, an on target intensity of $>10^{20}$ W/cm^2 was generated.

The primary proton diagnostics were RCF stacks, and 5 Thomson parabola spectrometers (TPS) positioned at various angles from target normal, with image plates used as the detector, as shown in figure 2 below. TPS are spectrometers consisting of an entry pinhole (of 250µm diameter in this case), a strong ~1T permanent magnet, and a pair of electric plates upon which a ~20kV potential difference is applied. The magnet deflects incoming ions vertically according to their energy, and the electric plates deflect them horizontally according to their charge/mass ratio.

These deflections, S_B and S_E respectively, are described in equations 3 and 4 below [9].

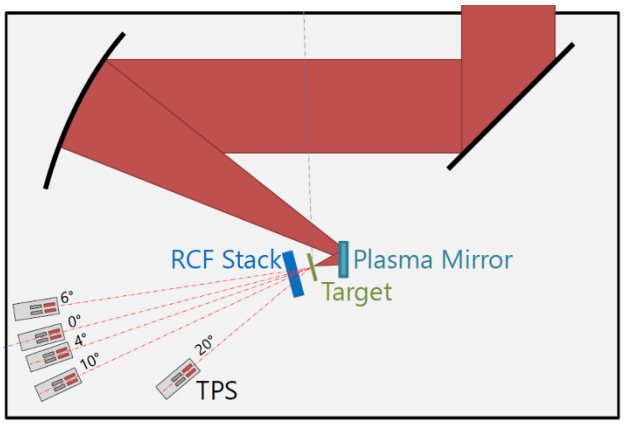

Figure 2: Experimental setup in TAP [2]

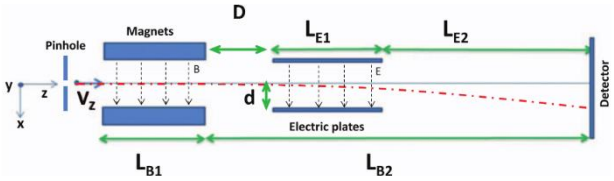

Figure 3: Setup of a typical Thomson parabola spectrometer

$$S_B = \alpha B\left(\frac{L_{B1}^2}{2} + L_{B1}L_{B2}\right) \quad (3)$$

$$S_E = \alpha^2 E\frac{m}{q}\left(\frac{L_{E1}^2}{2} + L_{E1}L_{E2}\right) \quad (4)$$

Where $\alpha = q/mv_z$ where q, m, and v_z are the charge, mass, and velocity of the ion respectively. L_{B1}, L_{B2}, L_{E1}, and L_{E2} are the distances shown in figure 3. The net effect of these two components is the generation of parabolic streaks of ions with distinct q/m values on the detector. This separation of species, coupled with the high energy resolution makes TPS a very useful diagnostic in ion acceleration experiments, where typically multispecies ion beams are produced.

Method

In order to calibrate the IPs for charged particles, CR-39 was used in conjunction with IPs to relate the PSL at a particular energy to the particle number. In the past, this has been done with slotted CR-39 placed in front of the IP, as in Doria *et al* [10]. This method works well for heavy ions, as in [10], however for protons, it will only work provided the proton tracks can be etched clearly, meaning they must stop in the CR-39. For 1mm thick CR-39, protons less than ~10 MeV will be stopped. In order to calibrate the IP for energies greater than this, a new method had to be developed. The CR-39 was placed behind the IP, with an iron or copper filter between the two, in order to slow the protons to ~10 MeV before interaction with the CR-39. The thickness of the filter determined the energy of protons stopping at the front and back surfaces of the CR-39. For each of the 5 TPS, a different filter was chosen, giving data points in a range of energies, determined by SRIM simulations [11], as described in the table below.

TP	Filter	Energy at front surface (MeV)	Energy at back surface (MeV)
-6°	500 Cu	17.6	21.3
0°	1250 Cu	27.4	30.2
4°	2500 Fe	38.1	40.3
10°	250 Cu	13.2	17.6
20°	2 IP	11.1	15.9

In the TPS at 20° the filter was a second image plate. This was to determine experimentally the stopping power of an image plate, to insert into the SRIM simulations for the subsequent TPS. After etching the CR-39, the first proton pits to be visible under a microscope are those whose Bragg peaks were reached at or close to the front and back surfaces. This gave two energy bins for every CR-39 used, in the form of 2 "streaks" of pits such as the one shown in figure 5 below. The width of these energy bins were determined after counting the pits by measuring the length along the streak counted, and knowing the energy at the surface, using equations 3 and 4 to calculate the energy further up the streak. This length was corrected for lateral scattering, according to SRIM. The sum of the PSL after background subtraction on the IP in that energy bin was then related to the total particle number, and a calibration curve relating PSL/proton and energy was created.

Experimental Results

Shown on figure 4 is the scanned image plate from TP1, which is then converted to a background subtracted PSL spectrum. The proton and carbon 6+ tracks are clearly visible.

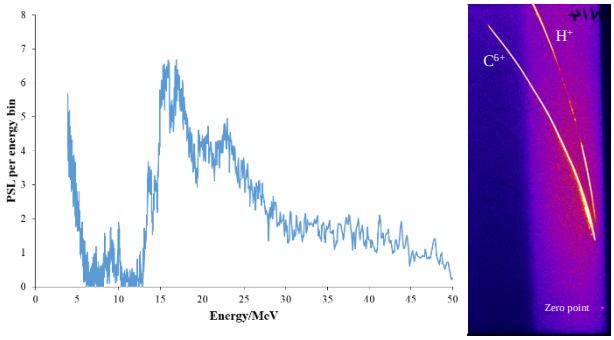

Figure 4: Raw IP image showing proton and carbon 6+ traces, with the PSL spectrum derived from proton trace

After etching the CR-39, images were taken of the pits at ×20 magnification, and stitched together to form a complete image of one proton streak, before the individual pits were counted up to the point where they became too faint to distinguish. Noise per unit area far away from the proton signal was counted and subtracted from the total number of pits, although this was negligible compared to the number of protons.

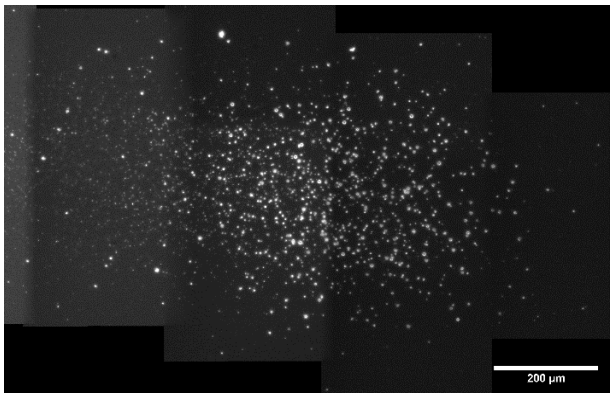

Figure 5: Image of pits on CR-39 front surface from TP0°

The total PSL for the energy bin represented by the streak was calculated, and the resulting calibration curve was plotted and compared to calibrations taken from references [5] and [6] in figure 6 below. Note that those curves are extrapolations from 20 MeV up for Mančić, and back from 80 MeV for Rabhi.

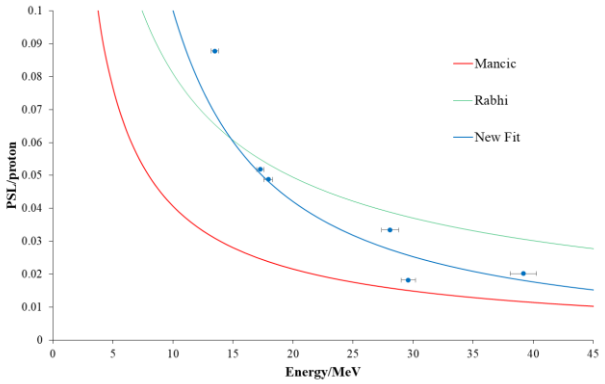

Figure 6: PSL per proton calibration curve

The new calibration can be seen to be broadly consistent with the two previous calibrations within the energy range investigated, albeit with a steeper trend. The new fit is represented by the power law,

$$\frac{PSL}{p^+} = 1.78E^{-1.25} \quad (5)$$

Where E is the energy in MeV of the proton incident on the image plate. This calibration was applied to the PSL spectrum shown in figure 4 to determine a final proton number per MeV, and knowing the pinhole diameter of the TPS, a final particle per MeV per steradian value can be determined. The resulting spectrum was compared to a spectrum obtained using the calibration from Mančić *et al*.

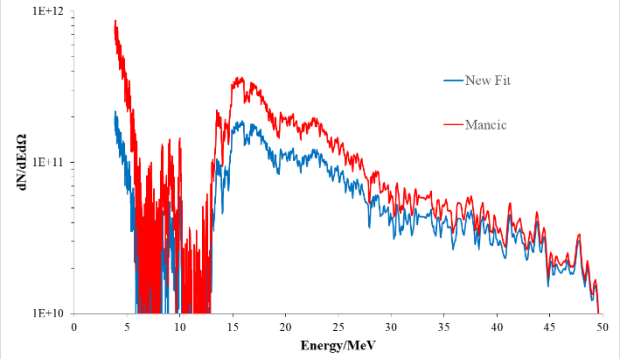

Figure 7: Comparison of proton spectra obtained with the two different calibration curves

As can be seen, the calibrations remain broadly consistent within the same order of magnitude, with better agreement at high proton energies. This implies this new calibration works well for high energies, which is especially useful in laser acceleration experiments where proton energies >30 MeV are routinely produced from most high power laser systems.

Conclusions

The response of Fujifilm BAS-TR image plates has now been calibrated using laser accelerated protons up to 40 MeV, extending the previous calibration from laser accelerated protons from 20 MeV, and filling the gap in the calibration which existed from 20-80 MeV. The calibrations previously were extrapolated, while our new calibration is a direct confirmation. The response was in the form of a power law, as expected and in agreement with those previously reported. The final spectrum obtained from this new calibration was found to agree with that from [5] within the same order of magnitude and may be used to determine proton spectra from future high energy laser driven acceleration experiments.

Acknowledgements

The authors acknowledge facility access provided by the Science and Technology Facility Council and grant funding from the Engineering and Physical Sciences Facility Council (grant EP/K022415/1). The authors also acknowledge support from the laser and technical staff and target fabrication group at the Rutherford Appleton Laboratory.

References

1. Bonnet *et al.* Rev. Sci. Instrum. **84**, 013508 (2013)
2. A. Alejo, Thesis QUB (2017)
3. Fujifilm IP scanner user manual, page 52 (http://beamline.harima.-riken.jp/bl45xu/web_old/Info/BAS2500img Spec.pdf)
4. Alejo *et al.* Rev. Sci. Instrum. **85**, 093303 (2014)
5. Mančić *et al.* Rev. Sci. Instrum. **79**, 073301 (2008)
6. Rabhi *et al.* Rev. Sci. Instrum. **88**, 113301 (2017)
7. Kar *et al.* J. Appl. Phys. **101**, 044510 (2007)
8. Kar *et al*., Phys. Rev. Letts. **109**, 185006 (2012)
9. Gwynne *et al.* Rev. Sci. Instrum. **85**, 033304 (2014)
10. Doria *et al.* Rev. Sci. Instrum. **86**, 123302 (2015)
11. J. F. Ziegler and J. P. Biersack, http://www.srim.org, 2003